Surface and deep ocean coupling in the subpolar North Atlantic during the last 230 years

I. R. Hall,[1] K. P. Boessenkool,[1] S. Barker,[1] I. N. McCave,[2] and H. Elderfield[2]

[1]   The subpolar North Atlantic Ocean (SPNA) is of key importance for modulating the climate of NW Europe because of heat loss to the atmosphere from the North Atlantic Current. Although hydrographic properties of the surface SPNA vary on interannual to multidecadal timescales, hydrographic time series scarcely extend back beyond the 1950s. We present a 230 year long record of SPNA surface conditions reconstructed from a very high accumulation rate core that also registers changes in deep flow speed in the Iceland Basin. A lagged correlation is observed between the records of deep flow speed and stable oxygen isotopic composition of the surface SPNA ($\delta^{18}O_w$), with strongest correlation when the paleoflow speed record leads by 15–20 years. This offset may to some extent reflect size-selective biological mixing of the sediment. Nonetheless, these records reveal a decadal-scale coupling between surface and deep ocean variability over the past 230 years, possibly driven by the North Atlantic Oscillation, with implications for North Atlantic circulation and climate.

1. Introduction

[2]   Surface circulation in the subpolar North Atlantic Ocean (SPNA) occurs in the subpolar gyre, which circulates cyclonically between 50°N and 65°N, and which contains strong boundary currents [*Hakkinen and Rhines*, 2004] (Figure 1). The subpolar front develops along the gyre's eastern boundary in the Iceland Basin where it meets the North Atlantic Current (NAC) [*Flatau et al.*, 2003]. Interannual variability occurs primarily through interactions with the atmosphere. Large-scale ocean circulation, including deep circulation, has been suggested as a cause for multidecadal variability in SPNA surface properties on the basis of observational time series of surface and deep hydrography, as well as through comparison with circulation models. Interannual variability of circulation and temperature in the surface SPNA is intimately linked to the North Atlantic Oscillation (NAO) [*Cayan*, 1992; *Curry and McCartney*, 2001; *Curry and Mauritzen*, 2005; *Flatau et al.*, 2003; *Marshall et al.*, 2001]. Its atmospheric component is characterized by a sea level pressure (SLP) dipole between the Azores high and Icelandic low, and expressed as an index of the normalized SLP difference between these areas [*Jones et al.*, 1997]. Relative to "low-index" phases, "high-index" NAO years in the North Atlantic region are characterized by (1) a stronger atmospheric meridional pressure gradient with stronger westerlies and northward displacement of the storm track; (2) more intense subpolar gyre (SPG) circulation [*Curry and McCartney*, 2001; *Curry and Mauritzen*, 2005; *Flatau et al.*, 2003; *Hakkinen and Rhines*, 2004]; (3) an eastward displacement of the subpolar front and intensified zonal sea surface temperature (SST) gradients [*Flatau et al.*, 2003]; (4) increased zonal advection that cools most of the SPNA, especially the area between 50°N and 60°N, by up to 0.5°C per month [*Cayan*, 1992; *Flatau et al.*, 2003]; and (5) freshening of the SPNA due to increased precipitation [*Walsh and Portis*, 1999] and/or advection [*Brauch and Gerdes*, 2005].

[3]   The poleward flux of warm saline Atlantic waters of the NAC constitutes the main surface branch of the Atlantic Meridional Overturning Circulation (AMOC) [*Cunningham et al.*, 2007; *Curry and Mauritzen*, 2005], which has been shown to vary on subannual [*Cunningham et al.*, 2007] to millennial [*Bianchi and McCave*, 1999; *Thornalley et al.*, 2009] timescales. Major AMOC reorganizations potentially have a large impact on regional and global climate [*Vellinga and Wood*, 2002]. The deep, equatorward limb of the AMOC consists of lower and upper North Atlantic Deep Water (NADW), originating from dense water masses formed in the Nordic Seas and the Labrador Sea, respectively (Figure 1). Some of the Nordic Seas dense water overflows the Greenland-Scotland ridges through Denmark Strait, while another part exits between Iceland and Scotland to enter the Iceland Basin as Iceland-Scotland Overflow Water (ISOW). In the Labrador Sea, high-NAO winters, and especially several consecutive winters with a high NAO index, lead to increased volume and depth of convection [*Dickson et al.*, 1996], and produce anomalously cold, fresh

[1]School of Earth and Ocean Sciences, Cardiff University, Cardiff, UK.
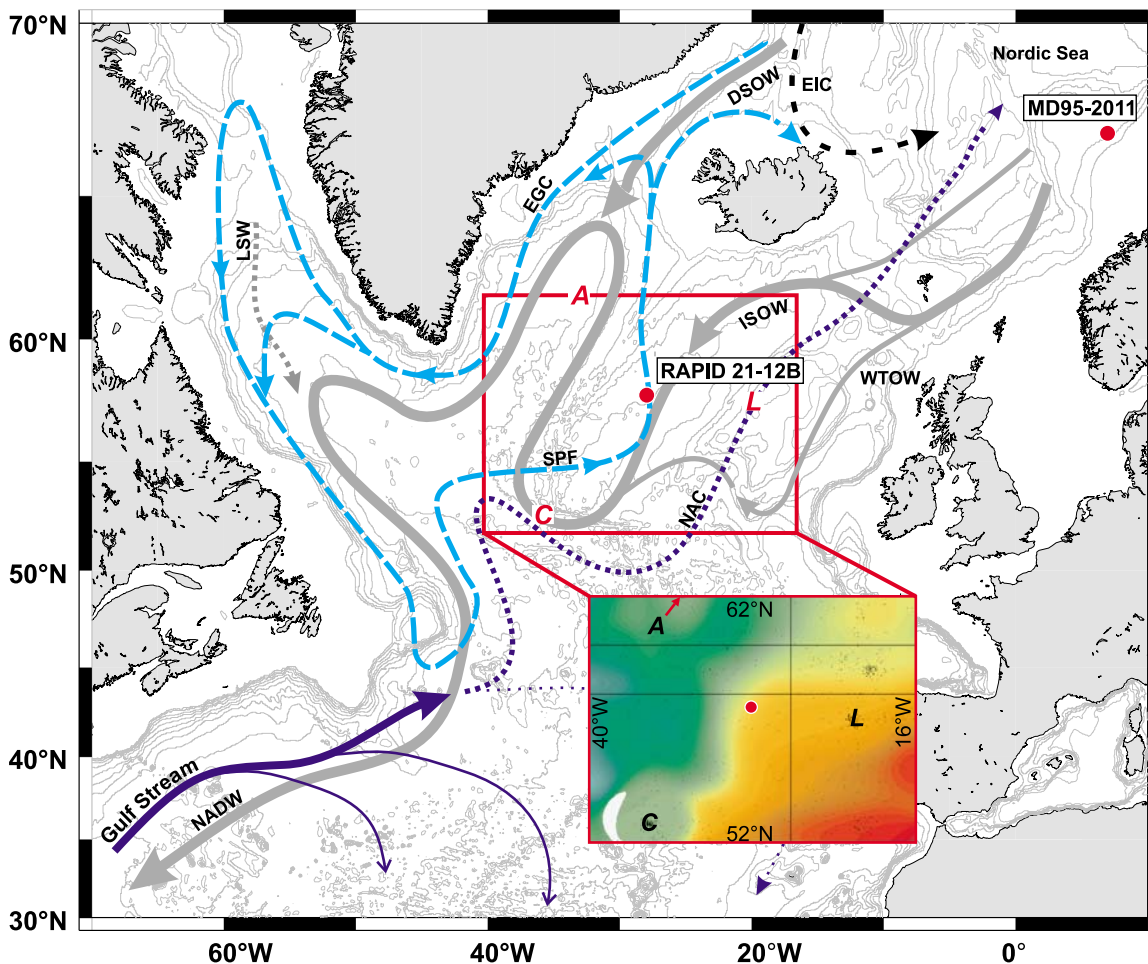[2]Department of Earth Sciences, University of Cambridge, Cambridge, UK.

Figure 1. Study area with generalized circulation of surface (blue dashed) and deep (gray solid) water masses [*Mauritzen*, 1996]. NAC, North Atlantic Current; EGC, East Greenland Current; SPF, Subpolar Front; ISOW, Iceland Scotland Overflow Water; DSOW, Denmark Strait Overflow Water; LSW, Labrador Sea Water; NADW, North Atlantic Deep Water. Also shown are the locations of cores RAPID-21-12B and MD95-2011 [*Andersson et al.*, 2003; *Risebrobakken et al.*, 2003]. Core 12B is located on the central Gardar Drift, a ~1100 km long sedimentary body presently lying under the main pathway of the deep western boundary current of ISOW in the Iceland Basin [*Bianchi and McCave*, 2000]. The boundary between the subpolar and warm Atlantic waters is roughly defined by the position of the SPF, which is apparent in the average sea surface temperature (SST) pattern for May–August of 1947–2003 in the area indicated with the red box [*Boyer et al.*, 2006] (see Figure 3 for legend). A, C, and L are the locations of ocean weather stations Alpha, Charlie, and Lima.

and dense Labrador Sea Water "vintages," such as that of 1993–1994 [*Yashayaev et al.*, 2007]. These waters are exported and, within 2–5 years of their formation, can be traced throughout the subpolar North Atlantic at intermediate depths [*Yashayaev et al.*, 2007], where they can influence the composition and flow speed of underlying water masses, such as ISOW [*Boessenkool et al.*, 2007; *Dickson et al.*, 2002].

[4] We present reconstructions of sea surface temperature (SST) and stable oxygen isotopic composition of the surface waters ($\delta^{18}O_w$) coregistered in the same samples of core 12B for which grain size proxy data for flow speed have been reported previously [*Boessenkool et al.*, 2007]. These

are based on Mg/Ca paleothermometry and the stable oxygen isotope composition of the tests of the surface-dwelling planktonic foraminifera *Globigerina bulloides*.

2. Materials and Methods

2.1. Sediment Core 12B

[5] High-resolution sediment box core RAPiD-21-12B (hereafter core 12B; 57°27.09′N, 27°54.53′W; 2630 m water depth) from the SPNA [*Boessenkool et al.*, 2007] offers a unique opportunity to further explore the relationship between interdecadal and multidecadal variations in SPNA surface hydrography and deep ocean circulation during the

last 230 years. The core was recovered from Gardar Drift on the eastern flank of Reykjanes Ridge where the interaction of ISOW with the underlying seafloor topography results in sediment focusing and enhanced sedimentation rates.

[6] Core 12B was subsampled at 0.5 cm resolution. The sediment samples were washed over a 63 μm mesh sieve using deionized water. Both filtrate and residue were left to settle, and, after decantation of the supernatant water, dried at 40°C. The <63μm fraction was used for grain-size analysis [Boessenkool et al., 2007], the >63μm fraction was dry sieved to obtain the 250–355 μm fraction. Specimens of foraminifera were hand picked from the narrowest size fraction possible (250–315 μm) for stable oxygen and Mg/Ca paleothermometry. Care was taken that the specimens were as clean as possible, morphologically consistent and the least corroded. Low numbers of G. bulloides (11 specimens of the analyzed size fraction per gram of dry bulk sediment compared to an average of 43 specimens per gram throughout the core) were present between 1.0 and 2.5 cm core depth. The sample 1.0–1.5 cm did not contain enough specimens of G. bulloides for both analyses and was therefore not analyzed for Mg/Ca.

2.2. Stable Isotope Analysis

[7] Eight specimens of G. bulloides were selected for stable oxygen and carbon isotope analysis. They were cleaned using 5% hydrogen peroxide for 30 min, followed by a methanol rinse, including 1s in an ultrasonic bath. They were oven dried at 40°C before analysis on a Thermo-Finnigan MAT252 mass spectrometer with a Kiel-type carbonate preparation device, and a long-term external reproducibility ≤0.08‰.

2.3. Mg/Ca Analysis

[8] Between 12 and 33 specimens (20 on average) of G. bulloides were selected for Mg/Ca analysis. They were cleaned for Mg/Ca analysis following [Barker et al., 2003] and analyzed on an ICP-AES (Varian Vista) with a precision better than 0.4% (1σ; liquid standard), and sample reproducibility of ≤4%. The first batch of samples included all but one of the core's samples (n = 108), they were run in order from top to bottom. For all but the upper four analyzed samples (0–2.25 cm), an extra centrifuge step was added after treatment with the oxidizing agent to improve recovery rates. Four analyses from the first run were discarded because of very low recovery rates (Ca concentrations < 10 ppm; samples 15.25 cm and 33.75 cm), probable contamination (Fe/Mg > 0.1 mol/mol; sample 52.75 cm), or a value outside the 3-sigma range of the entire data set (sample 31.75 cm). A second batch (n = 37) consisted of new foraminifer subsamples from selected levels, especially where recoveries were low in the first batch. None of these duplicates were discarded, and all samples were used separately in further calculations (no averages were taken for duplicates). The difference between duplicate measurements was 0.256 mmol/mol Mg/Ca on average, and up to 0.964 mmol/mol, which would equate to a difference in calcification temperature of approximately 4.0°C.

2.4. Mg/Ca Calcification Temperatures and Oxygen Isotopic Composition of Seawater

[9] To reconstruct calcification temperatures over the studied interval the Mg/Ca-temperature relationship of Barker and Elderfield [2002] was used: Mg/Ca = 0.72 * $e^{0.1T}$, where Mg/Ca is the elemental ratio in foraminiferal calcite in mmol/mol, and T is the calcification temperature in °C. Together with the $\delta^{18}O_c$ results, these Mg/Ca-based calcification temperatures were used to reconstruct changes in the oxygen isotopic composition of seawater ($\delta^{18}O_w$) using the paleotemperature equation for 12-chambered G. bulloides [Bemis et al., 1998]. Uncertainty on the Mg/Ca temperature calibration is on the order 1.2°C–1.3°C [Anand et al., 2003; Lea et al., 1999]. However, any error here will be systematic for all samples and will therefore have limited effect on the overall structure of the resulting temperature or $\delta^{18}O_w$ records. Analytical errors, as described above, were propagated to provide a 1-sigma uncertainty envelope on the derived $\delta^{18}O_w$ estimates.

2.5. Age Model

[10] Sediment box core 12B was recovered in 2004. It covers the period 1770–2004 A.D., based on ^{210}Pb geochronology, which indicates maximum sediment accumulation rates of 2.3 ± 0.2 mm a^{-1} [Boessenkool et al., 2007]. This age model is based on the assumption that the ^{210}Pb profile is driven by sedimentation only. Because ^{210}Pb is adsorbed mainly onto clays the age profile is for the fine fraction.

3. Results and Discussion

[11] Both the G. bulloides $\delta^{18}O_c$ and Mg/Ca records of core 12B show a large amount of scatter (Figures 2a and 2b), that is not as evident in the August SST estimates based on fossil diatom assemblages at the site [Miettinen et al., 2010]. There is very little evidence for dissolution of foraminifer test calcite (bar some dissolution in the upper 2 cm of the core), making it very unlikely that this is a major cause for the scatter in the Mg/Ca record [Brown and Elderfield, 1996]. G. bulloides has a predominantly subpolar habitat [Bé and Tolderlund, 1971], and modern core top data from the North Atlantic show a clear temperature limitation on the distribution with sharply decreasing abundances below SST of 7°C–8°C [Farmer et al., 2008]. While production may vary as a function of latitude, G. bulloides in the subpolar region is suggested to reflect surface conditions, above the thermocline, occurring during the late spring to summer [Chapman et al., 2000; Duplessy et al., 1992; Elderfield and Ganssen, 2000; Schiebel et al., 1997]. We suggest the scatter in the $\delta^{18}O_c$ and Mg/Ca data probably reflects the large seasonal variation in hydrographic properties in the region and the proximity of the subpolar front (Figures 1 and 3), whose positional shifts give SST changes of ~3°C during the spring-summer season. Interannual variability in the timing of the occurrence or calcification of G. bulloides [Tolderlund and Bé, 1971] could also play a role, as could genetic variability [Stewart et al., 2001], and variations in calcification depth. Average spring-summer hydrographic data (1947–2003) for the area 52°N–62°N,
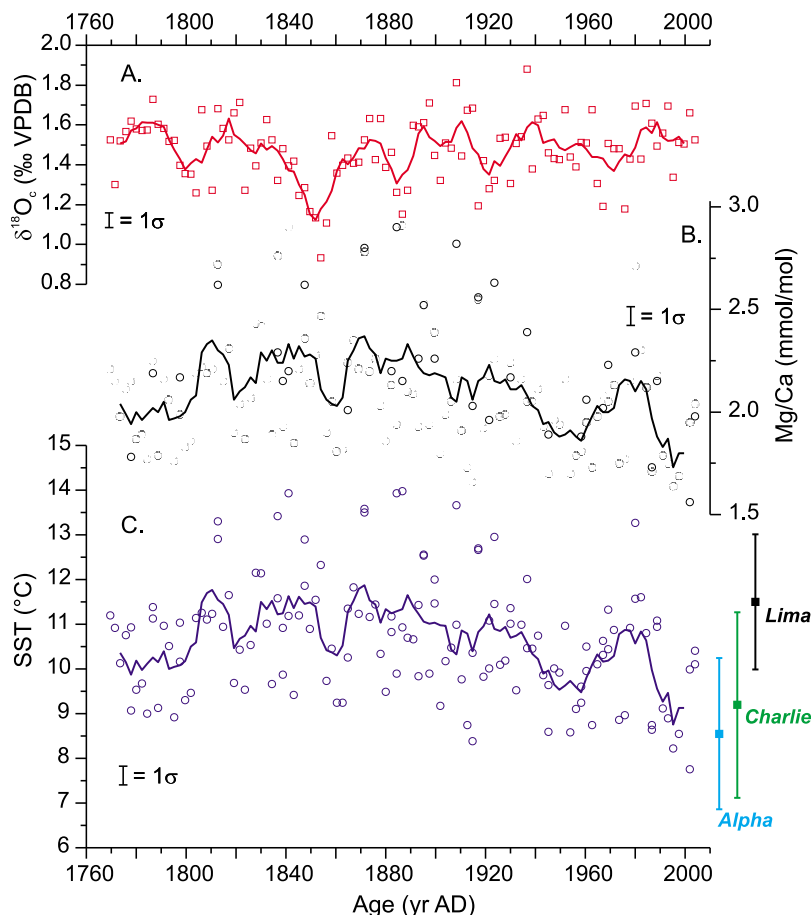
Figure 2. Paleoceanographic surface ocean records of the planktonic foraminifera *Globigerina bulloides* in core 12B. Lines are five-point moving averages. (a) Stable oxygen isotope composition ($\delta^{18}O_c$), (b) Mg/Ca ratio, and (c) Mg/Ca-based calcification temperatures. The average calcification temperature is 10.6°C, and the total range is 6.2°C. Analytical error bars represent 1-sigma uncertainty. For comparison, the averages and 1-sigma ranges of the SST measured at three ocean weather stations are shown on the same *y* axis as Figure 2c. See Figure 1 for locations.

40°W–0°W at the surface and 50 m water depth (Figure 3) suggest that changes in the calcification depth of *G. bulloides* could introduce discrepancies between the calcification temperature and the SST of up to 2°C. Although, recent work by *Mekik et al.* [2007] showed that the strongest relationship between Mg/Ca and temperature occurred at 30 m water depth. While at sites with lower sediment accumulation rates such scatter would be (partly) evened out by the larger integration time represented by individual samples, such natural smoothing is likely lessened due to the high sediment accumulation rates and 0.5 cm sampling at the site of core 12B. The $\delta^{18}O_c$ and Mg/Ca records (Figures 2a and 2b) were therefore smoothed using a simple five-point moving average (~11 years) prior to calculation of $\delta^{18}O_w$ values. This smoothing was chosen to minimize seasonal/interannual variability and emphasize decadal trends in both the SST and $\delta^{18}O_w$ reconstructions (Figure 4); both records show interdecadal to multidecadal variability over the past 230 years that can be compared to flow speed variations of ISOW in the deep subpolar North Atlantic, recorded as

changes in the mean grain size of the "sortable silt" (10–63 μm) fraction ($\overline{SS}$) in the same sediment samples [*Boessenkool et al.*, 2007] (Figure 4).

[12] Analysis of the phase relationship between the records of ISOW flow speed and $\delta^{18}O_w$ using the PearsonT program [*Mudelsee*, 2003], reveals a lag correlation with strongest positive correlation when $\overline{SS}$ leads $\delta^{18}O_w$ by 15–20 years. This offset may represent a real lagged response of the surface Subpolar North Atlantic to changes in the overturning circulation, perhaps through changes in formation of subpolar intermediate water masses (i.e., LSW [cf. *Boessenkool et al.*, 2007]). However, in this region, as in others where deep water is formed, signals are typically transmitted from surface to depth; with downstream deep flow and properties lagging upstream surface conditions. For example there is a 3 year lag between conditions in the top 500 m at Fram Strait and at 2000 m in the core of the Denmark Strait overflow off SE Greenland [*Dickson et al.*, 1999]. An additional year's delay links these conditions with the deep DSOW layer in the Labrador Sea [*Dickson and*
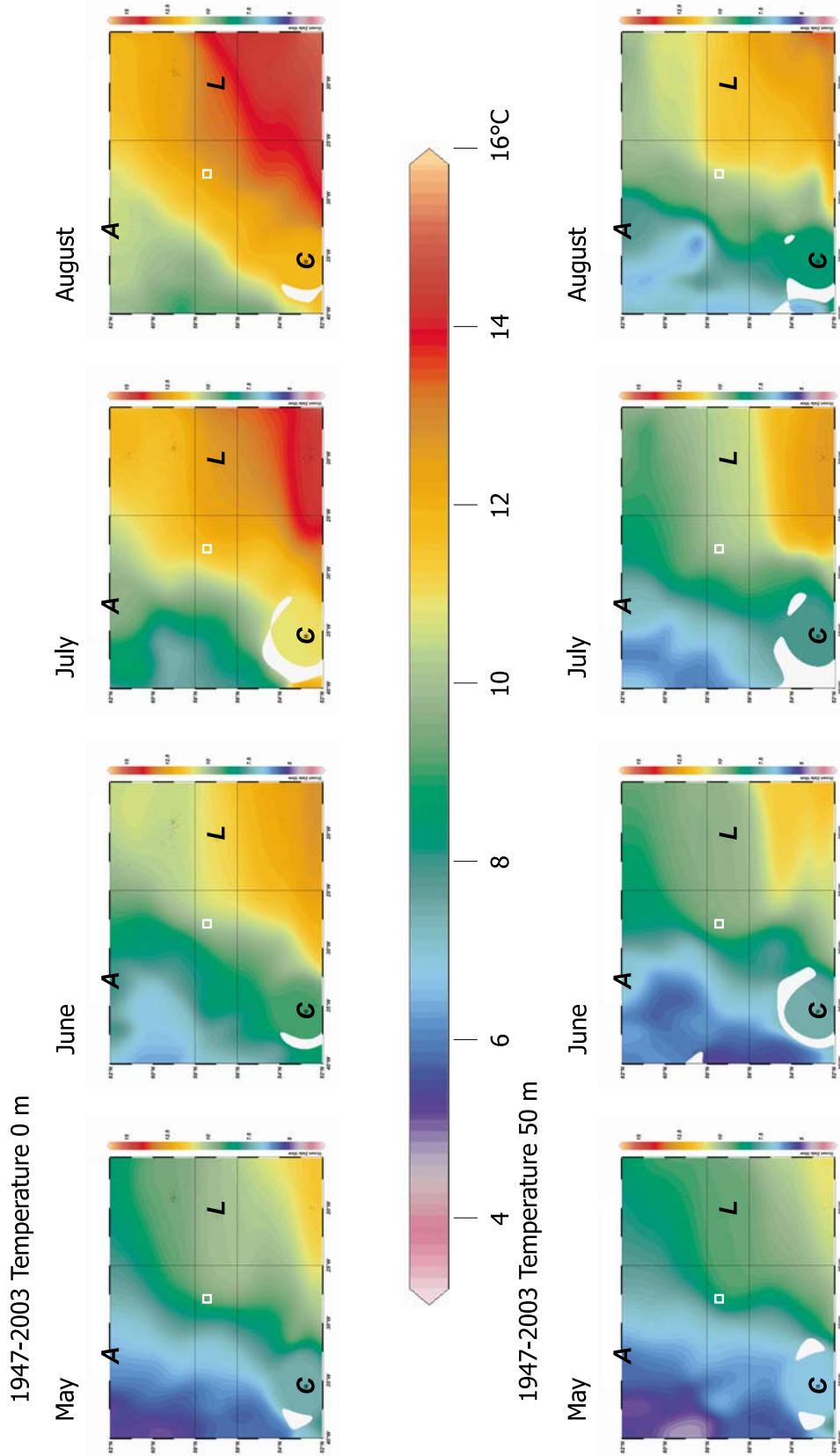
Figure 3. Average spring-summer hydrographic data (1947–2003) for the area 52°N–62°N, 40°W–0°W. Small square is core location of core 12B. Data from World Ocean Database 2005 [*Boyer et al.*, 2006] are plotted using Ocean Data View (R. Schlitzer, 2006, available at http://odv.awi.de) with gridding length 100 km. Temperatures at (top) 0 m and (bottom) 50 m water depth.
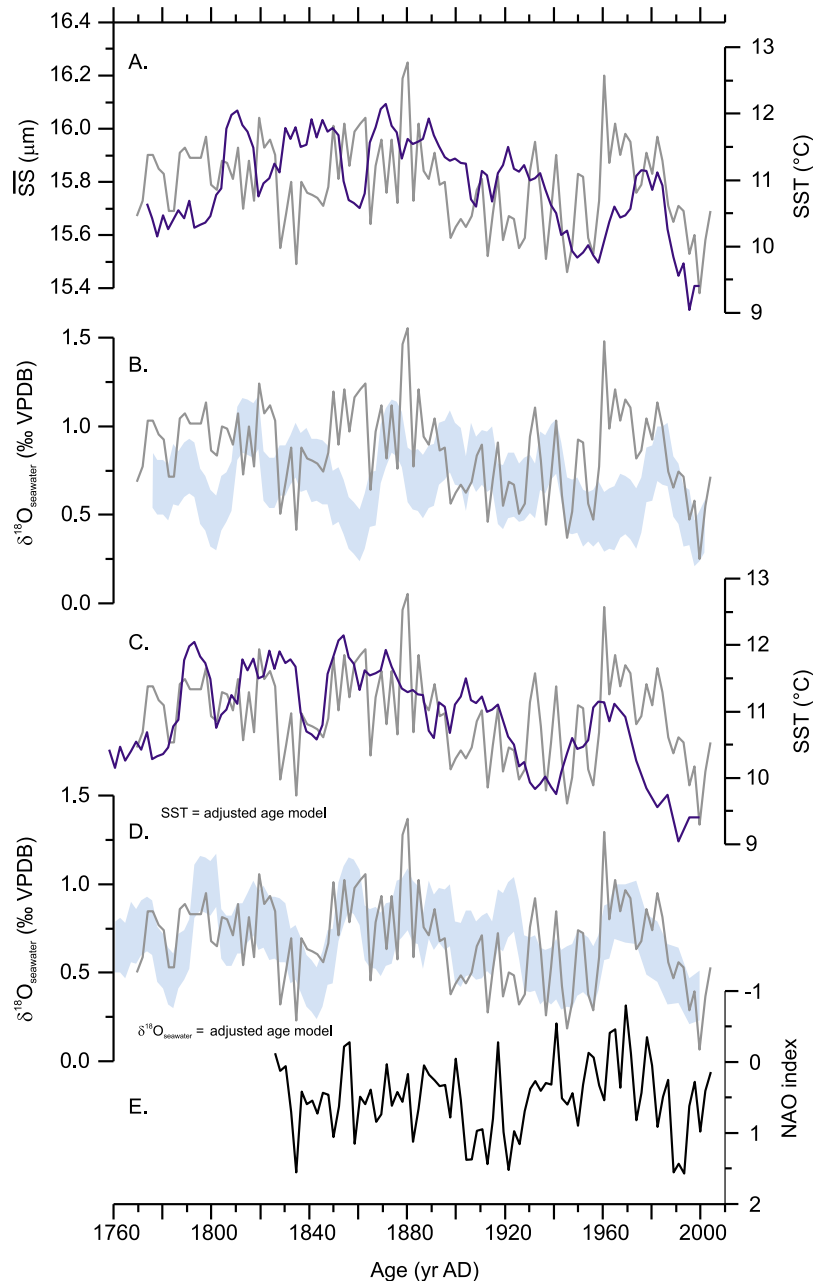
Figure 4. (a–d) Combined paleoceanographic records of surface and deep ocean change from core 12B. The mean grain size of the "sortable" (10–63 μm) silt fraction ($\overline{SS}$) on original age model [*Boessenkool et al.*, 2007] in gray (in Figure 4a and copied in Figures 4b–4d) indicates multidecadal changes in the deep flow speed of ISOW over the eastern flank of Reykjanes Ridge. Dark blue line (Figures 4a and 4c) is Mg/Ca-based reconstruction of SST; light blue shading is the reconstructed oxygen isotopic composition of the surface seawater ($\delta^{18}O_w$) calculated using $\delta^{18}O_c$ and Mg/Ca-based SSTs (see section 2), including propagated analytical (1 sigma) errors (Figures 4b and 4d). Surface data on original age model shown in Figures 4a and 4b and on "adjusted age model" incorporating a 17.4 year older shift of SST and $\delta^{18}O_w$ shown in Figures 4c and 4d. (e) The NAO data used by *Boessenkool et al.* [2007] for comparison.

Meincke, 2003; *Visbeck et al.*, 2003] (who also show several other NAO-related sequential changes in the North Atlantic). Thus a decadal-scale lead of deep ISOW flow over the surface would seem highly anomalous.

[13] An alternative explanation that we cannot rule out is that the apparent offset could be an artifact introduced by biological separation of simultaneously deposited fine and coarse sediment size fractions. Absence of lamination and presence of some pockets of fecal pellets in core 12B show
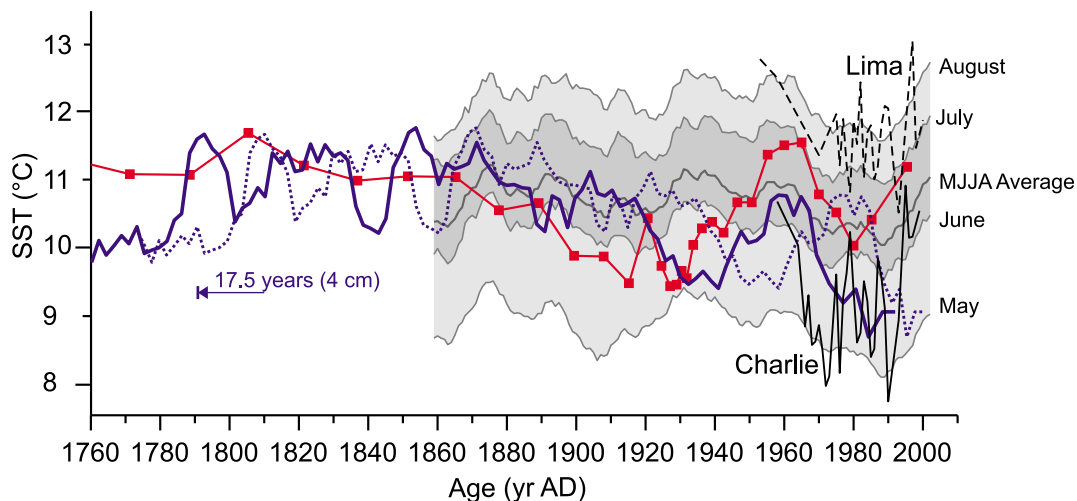
Figure 5. Comparison of sea surface temperature (SST) records. The blue dotted line is core 12B Mg/Ca-based SST estimates on original age model [*Boessenkool et al.*, 2007]. The blue solid line is the Mg/Ca-based SST estimates on adjusted age model. The red solid line is the foraminiferal assemblage based SST estimates for summer (JAS) for site MD95-2011 [*Andersson et al.*, 2003; *Risebrobakken et al.*, 2003]. Gray lines are SST for location 58°N, 28°W from NCDC Extended Reconstruction SST (ERSST.v2) [*Smith and Reynolds*, 2004]; data smoothed using 11 year moving average. Black lines are SST from ocean weather stations Charlie (solid) and Lima (dashed) [*Boyer et al.*, 2006].

that its sediments have been mixed by bioturbating organisms. Sediment cores from other sites on the drift also show clear signs of bioturbation [*Bianchi and McCave*, 2000]. Apparent leads and lags can be introduced in sedimentary records by nondiffusive size-dependent mixing of particles in the sediment column. Burrowing activity, combined with decreasing sediment shear strength toward the sediment-water interface, has been inferred to be responsible for gravel-sized rock fragments being advected ("pumped") upward and maintained at or near the surface in deep-sea sediments off Nova Scotia [*McCave*, 1988]. This mechanism has also been held responsible for offsets in ^{14}C ages between foraminiferal and fine (coccolith) fraction carbonate [*Brown et al.*, 2001; *Thomson et al.*, 1995]. With meiofaunal-sized burrowers [*Thistle and Sherman*, 1985], this process could potentially also affect foraminifera of the >250 μm size fraction and would cause foraminifera larger than 250 μm at any depth in the core to be older than the fine (<63 μm) fraction at the same level. A 17.4 year apparent age difference between foraminifera and muds at the same level in core 12B would equate to a relative movement between size classes of 4 cm. That would involve an advective velocity of 0.23 cm a^{-1}, at the lower end of bioadvective rates (0.12–27 cm a^{-1}, albeit downward) measured in modern shallow sediments [*Gerino et al.*, 2007]. Advection of fines is unlikely to be the cause as this normally involves addition of old carbon, rendering the fines older than the foraminifera [*Keigwin et al.*, 1984; *Ohkouchi et al.*, 2002]. Unfortunately, the low abundance of foraminifera (as noted above) precludes ^{14}C analyses in the surface layer of this high accumulation rate site.

[14] Figures 4c and 4d show the SST and $\delta^{18}O_w$ reconstructions using an adapted age model that takes size

differential mixing into account; the *adjusted age model* applies only to the >250 μm fraction, which comprises less than 5% of the total sediment dry weight at any level in the core. It introduces a constant offset of 17.4 year (equivalent of 4 cm in the sediment column) to the above age model to all samples except those in the upper 4 cm. For the records to end at the same time as the original age model (A.D. 2004), the ages for the top 4 cm were linearly interpolated between 1965 and 2004. Using the adjusted age model for the >250 μm fraction (i.e., the $\delta^{18}O_w$ record) and the original age model for the fine sediment fraction (i.e., the $\overline{SS}$ record), Pearson's r for the correlation between the $\overline{SS}$ and $\delta^{18}O_w$ records is 0.40, with a 95% confidence interval of [0.24; 0.52] (n = 99). Although significant, the correlation between the $\overline{SS}$ record (on the original age model) and SST record (on the adjusted age model) is less strong (Pearson's r of 0.21 [0.03; 0.36], n = 98). This might well be caused by a strong imprint of seasonal variations on the SST record, the amplitude of which is much larger than that of $\delta^{18}O_w$ in the SPNA. Support for a bioturbational offset is provided by the improved fit between the core 12B Mg/Ca based SST record when compared on the adjusted age model with historical SST time series and a high-resolution foraminiferal assemblage-based august SST reconstruction from Voring Plateau in the Nordic Seas [*Andersson et al.*, 2003; *Risebrobakken et al.*, 2003] located within the NAC, when compared on the adjusted age model (Figures 1 and 5). It should be emphasized that we have made the simplest assumption of a constant offset between the foraminifera and $\overline{SS}$ time series. These relationships appear even stronger when the 12B Mg/Ca based SST is directly correlated with the historical SST time series within the age uncertainty.

[15] The temperature record of Figure 4c displays a roughly periodic variation of 35–50, averaging ~42, years. While this is broadly consistent with NAO data of the last 130 years, it must be noted that the NAO is defined on pressure difference between two fixed locations, yet the centers of pressure move, and modern analyses of the short record that does exist do not find any clear multidecadal periodicity [*Hurrell and Deser*, 2009]. Nevertheless, our time series of Mg/Ca based SST and derived $\delta^{18}O_w$ may reveal coordinated climatic behavior.

4. Conclusions

[16] Our data suggest that changes in deep flow speed and the $\delta^{18}O_w$ of the surface SPNA (salinity) are coordinated on interdecadal to multidecadal timescales over the past 230 years. The deep flow speed changes recorded in SS at the core 12B location are largely related to varying production of LSW [*Boessenkool et al.*, 2007], which has been linked to variability of the SPG dynamics [*Hakkinen and Rhines*, 2004; *Lohmann et al.*, 2009; *Thornalley et al.*, 2009] and, among other forcing mechanisms, to the NAO [*Dickson et al.*, 1996; *Dickson et al.*, 2000]. Such a rela-

tionship would suggest an increase in LSW production is related to a decrease in ISOW flow and decrease in surface salinity, and vice versa, at the core 12B site. This is consistent with the suggestion of a dipole in convection between the Labrador Sea and the Nordic Seas [*Dickson et al.*, 1996]. The alternative, that there is a minimal size selective bioturbation effect, yields a potentially difficult to explain lagged (up to 15–20 years) relation of the surface ocean to changes in deep flow speed. This could reflect the rapid transfer of the NAO signal to the deep ocean via Labrador Seawater production [*Boessenkool et al.*, 2007], but also requires subsequent adjustment of the surface circulation in the subpolar gyre with respect to salinity. We regard this as less plausible, and suggest the bioturbation offset and convection dipole is more likely.

References

Anand, P., H. Elderfield, and M. H. Conte (2003), Calibration of Mg/Ca thermometry in planktonic foraminifera from a sediment trap time series, *Paleoceanography*, *18*(2), 1050, doi:10.1029/2002PA000846.

Andersson, C., B. Risebrobakken, E. Jansen, and S. O. Dahl (2003), Late Holocene surface ocean conditions of the Norwegian Sea (Vøring Plateau), *Paleoceanography*, *18*(2), 1044, doi:10.1029/2001PA000654.

Barker, S., and H. Elderfield (2002), Foraminiferal calcification response to glacial-interglacial changes in atmospheric CO_2, *Science*, *297*, 833–836, doi:10.1126/science.1072815.

Barker, S., M. Greaves, and H. Elderfield (2003), A study of cleaning procedures used for foraminiferal Mg/Ca paleothermometry, *Geochem. Geophys. Geosyst.*, *4*(9), 8407, doi:10.1029/2003GC000559.

Bé, A. W. H., and D. S. Tolderlund (1971), Distribution and ecology of living planktonic foraminifera in surface waters of the Atlantic and Indian oceans, in *The Micropaleontology of the Oceans*, edited by B. M. Funnell and W. R. Riedel, pp. 105–149, Cambridge Univ. Press, Cambridge, U. K.

Bemis, B. E., H. J. Spero, J. Bijma, and D. W. Lea (1998), Reevaluation of the oxygen isotopic composition of planktonic foraminifera: Experimental results and revised paleotemperature equations, *Paleoceanography*, *13*(2), 150–160, doi:10.1029/98PA00070.

Bianchi, G. G., and I. N. McCave (1999), Holocene periodicity in North Atlantic climate and deep-ocean flow south of Iceland, *Nature*, *397*, 515–517, doi:10.1038/17362.

Bianchi, G. G., and I. N. McCave (2000), Hydrography and sedimentation under the deep western boundary current on Björn and Gardar drifts, Iceland Basin, *Mar. Geol.*, *165*, 137–169, doi:10.1016/S0025-3227(99)00139-5.

Boessenkool, K. P., I. R. Hall, H. Elderfield, and I. Yashayaev (2007), North Atlantic climate and deep-ocean flow speed changes during

the last 230 years, *Geophys. Res. Lett.*, *34*, L13614, doi:10.1029/2007GL030285.

Boyer, T. P., J. I. Antonov, H. E. Garcia, D. R. Johnson, R. A. Locarnini, A. V. Mishonov, M. T. Pitcher, O. K. Baranova, and I. V. Smolyar (2006), *World Ocean Database 2005* [DVDs], *NOAA Atlas NESDIS*, vol. 60, edited by S. Levitus, 190 pp., U.S. Gov. Print. Off., Washington, D. C.

Brauch, J. P., and R. Gerdes (2005), Response of the northern North Atlantic and Arctic oceans to a sudden change of the North Atlantic Oscillation, *J. Geophys. Res.*, *110*, C11018, doi:10.1029/2004JC002436.

Brown, L., G. T. Cook, A. B. MacKenzie, and J. Thomson (2001), Radiocarbon age profiles and size dependency of mixing in northeast Atlantic sediments, *Radiocarbon*, *43*(2B), 929–937.

Brown, S. J., and H. Elderfield (1996), Variations in Mg/Ca and Sr/Ca ratios of planktonic foraminifera caused by postdepositional dissolution: Evidence of shallow Mg-dependent dissolution, *Paleoceanography*, *11*(5), 543–551, doi:10.1029/96PA01491.

Cayan, D. R. (1992), Latent and sensible heat-flux anomalies over the northern oceans: Driving the sea-surface temperature, *J. Phys. Oceanogr.*, *22*(8), 859–881 doi:10.1175/1520-0485(1992) 022<0859:LASHFA>2.0.CO;2.

Chapman, M. R., et al. (2000), Sea surface temperature variability during the last glacial-interglacial cycle: Assessing the magnitude and pattern of climate change in the North Atlantic, *Palaeogeogr. Palaeoclimatol. Palaeoecol.*, *157*, 1–25, doi:10.1016/S0031-0182 (99)00168-6.

Cunningham, S. A., et al. (2007), Temporal variability of the Atlantic meridional overturning circulation at 26.5°N, *Science*, *317*, 935–938, doi:10.1126/science.1141304.

Curry, R., and C. Mauritzen (2005), Dilution of the northern North Atlantic Ocean in recent decades, *Science*, *308*, 1772–1774, doi:10.1126/science.1109477.

Curry, R., and M. McCartney (2001), Ocean gyre circulation changes associated with the North Atlantic Oscillation, *J. Phys. Oceanogr.*, *31*(12), 3374–3400 doi:10.1175/1520-0485 (2001)031<3374:OGCCAW>2.0.CO;2.

Dickson, B., et al. (1999), Possible predictability in overflow from the Denmark Strait, *Nature*, *397*, 243–246, doi:10.1038/16680.

Dickson, B., et al. (2002), Rapid freshening of the deep North Atlantic Ocean over the past four decades, *Nature*, *416*, 832–837, doi:10.1038/416832a.

Dickson, R. R., and J. Meincke (2003), The North Atlantic Oscillation and the ocean's response in the 1990's, *ICES Mar. Sci. Symp.*, *219*, 15–24.

Dickson, R., et al. (1996), Long-term coordinated changes in the convective activity of the North Atlantic, *Prog. Oceanogr.*, *38*, 241–295, doi:10.1016/S0079-6611(97)00002-5.

Dickson, R. R., T. J. Osborn, J. W. Hurrell, J. Meincke, J. Blindheim, B. Adlandsvik, T. Vinje, G. Alekseev, and W. Maslowski (2000), The Arctic Ocean response to the North Atlantic Oscillation, *J. Clim.*, *13*(15), 2671–2696, doi:10.1175/1520-0442(2000) 013<2671:TAORTT>2.0.CO;2.

Duplessy, J. C., et al. (1992), Changes in surface salinity of the North Atlantic Ocean during the last deglaciation, *Nature*, *358*, 485–488, doi:10.1038/358485a0.

Elderfield, H., and G. Ganssen (2000), Past temperature and $\delta^{18}O$ of surface ocean waters inferred from foraminiferal Mg/Ca ratios, *Nature*, *405*, 442–445, doi:10.1038/35013033.

Farmer, E. J., M. R. Chapman, and J. E. Andrews (2008), Centennial-scale Holocene North Atlantic surface temperatures from Mg/Ca ratios in *Globigerina bulloides*, *Geochem. Geophys. Geosyst.*, *9*, Q12029, doi:10.1029/ 2008GC002199.

Flatau, M. K., et al. (2003), The North Atlantic Oscillation, surface current velocities, and SST changes in the subpolar North Atlantic,

J. Clim., *16*(14), 2355–2369, doi:10.1175/2787.1.

Gerino, M., M. Frignani, C. Mugnai, L. G. Bellucci, D. Prevedelli, A. Valentini, A. Castelli, S. Delmotte, and S. Sauvage (2007), Bioturbation in the Venice Lagoon: Rates and relationship to organisms, *Acta Oecol.*, *32*(1), 14–25, doi:10.1016/j.actao.2007.02.003.

Hakkinen, S., and P. B. Rhines (2004), Decline of subpolar North Atlantic circulation during the 1990s, *Science*, *304*, 555–559, doi:10.1126/science.1094917.

Hurrell, J. W., and C. Deser (2009), North Atlantic climate variability: The role of the North Atlantic Oscillation, *J. Mar. Syst.*, *78*(1), 28–41, doi:10.1016/j.jmarsys.2008.11.026.

Jones, P., et al. (1997), Extension to the North Atlantic Oscillation using early instrumental pressure observations from Gibraltar and south-west Iceland, *Int. J. Climatol.*, *17*, 1433–1450, doi:10.1002/(SICI)1097-0088(19971115)17:13<1433::AID-JOC203>3.0.CO;2-P.

Keigwin, L. D., et al. (1984), High-resolution isotope study of the latest deglaciation based on Bermuda Rise cores, *Quat. Res.*, *22*(3), 383–386, doi:10.1016/0033-5894(84)90031-0.

Lea, D. L., T. A. Mashiotta, and H. J. Spero (1999), Controls on magnesium and strontium uptake in planktonic foraminifera determined by live culturing, *Geochim. Cosmochim. Acta*, *63*(16), 2369–2379.

Lohmann, K., et al. (2009), Response of the North Atlantic subpolar gyre to persistent North Atlantic Oscillation like forcing, *Clim. Dyn.*, *32*(2–3), 273–285, doi:10.1007/s00382-008-0467-6.

Marshall, J., Y. Kushnir, D. Battisti, P. Chang, A. Czaja, R. Dickson, J. Hurrell, M. McCartney, R. Saravanan, and M. Visbeck (2001), North Atlantic climate variability: Phenomena, impacts and mechanisms, *Int. J. Climatol.*, *21*, 1863–1898, doi:10.1002/joc.693.

Mauritzen, C. (1996), Production of dense overflow waters feeding the North Atlantic across the Greenland-Scotland Ridge. Part 1: Evidence for a revised circulation scheme, *Deep Sea Res., Part I*, *43*(6), 769–806, doi:10.1016/0967-0637(96)00037-4.

McCave, I. N. (1988), Biological pumping upwards of the coarse fraction of deep-sea sediments, *J. Sediment. Petrol.*, *58*(1), 148–158.

Mekik, F., R. François, and M. Soon (2007), A novel approach to dissolution correction of Mg/Ca-based paleothermometry in the tropical Pacific, *Paleoceanography*, *22*, PA3217, doi:10.1029/2007PA001504.

Miettinen, A., N. Koç, I. R. Hall, F. Godtliebsen, and D. Divine (2010), North Atlantic sea surface temperatures and their relation to the North Atlantic Oscillation during the last 230 years, *Clim. Dyn.*, doi:10.1007/s00382-010-0791-5, in press.

Mudelsee, M. (2003), Estimating Pearson's correlation coefficient with bootstrap confidence interval from serially dependent time series, *Math. Geol.*, *35*(6), 651–665 doi:10.1023/B:MATG.0000002982.52104.02.

Ohkouchi, N., et al. (2002), Spatial and temporal offsets between proxy records in a sediment drift, *Science*, *298*, 1224–1227, doi:10.1126/science.1075287.

Risebrobakken, B., E. Jansen, C. Andersson, E. Mjelde, and K. Hevrøy (2003), A high-resolution study of Holocene paleoclimatic and paleoceanographic changes in the Nordic Seas, *Paleoceanography*, *18*(1), 1017, doi:10.1029/2002PA000764.

Schiebel, R., et al. (1997), Population dynamics of the planktic foraminifer *Globigerina bulloides* from the eastern North Atlantic, *Deep Sea Res., Part I*, *44*(9–10), 1701–1713, doi:10.1016/S0967-0637(97)00036-8.

Smith, T. M., and R. W. Reynolds (2004), Improved extended reconstruction of SST (1854–1997), *J. Clim.*, *17*(12), 2466–2477, doi:10.1175/1520-0442(2004)017<2466:IEROS>2.0.CO;2.

Stewart, I. A., et al. (2001), Genotypic variability in subarctic Atlantic planktic foraminifera, *Mar. Micropaleontol.*, *43*(1–2), 143–153, doi:10.1016/S0377-8398(01)00024-X.

Thistle, D., and K. M. Sherman (1985), The nematode fauna of a deep-sea site exposed to strong near-bottom currents, *Deep Sea Res., Part A*, *32*(9), 1077–1088.

Thomson, J., et al. (1995), Radiocarbon age offsets in different-sized carbonate components of deep-sea sediments, *Radiocarbon*, *37*(2), 91–101.

Thornalley, D. J. R., et al. (2009), Holocene oscillations in temperature and salinity of the surface subpolar North Atlantic, *Nature*, *457*, 711–714, doi:10.1038/nature07717.

Tolderlund, D. S., and A. W. H. Bé (1971), Seasonal distribution of planktonic foraminifera in the western North Atlantic, *Micropaleontology*, *17*(3), 297–329.

Vellinga, M., and R. A. Wood (2002), Global climatic impacts of a collapse of the Atlantic thermohaline circulation, *Clim. Change*, *54*, 251–267, doi:10.1023/A:1016168827653.

Visbeck, M., E. P. Chassignet, R. Curry, T. L. Delworth, R. R. Dickson, and G. Krahmann (2003), The ocean's response to North Atlantic Oscillation variability, in *The North Atlantic Oscillation: Climatic Significance and Environmental Impact*, *Geophys. Monogr. Ser.*, vol. 134, edited by J. W. Hurrell et al., pp. 113–145, AGU, Washington, D. C.

Walsh, J. E., and D. H. Portis (1999), Variations of precipitation and evaporation over the North Atlantic Ocean, 1958–1997, *J. Geophys. Res.*, *104*(D14), 16,613–16,631.

Yashayaev, I., M. Bersch, and H. M. van Aken (2007), Spreading of the Labrador Sea water to the Irminger and Iceland basins, *Geophys. Res. Lett.*, *34*, L10602, doi:10.1029/2006GL028999.

S. Barker, K. P. Boessenkool, and I. R. Hall, School of Earth and Ocean Sciences, Cardiff University, Main Building, Park Place, Cardiff CF10 3YE, UK. (hall@cardiff.ac.uk)

H. Elderfield and I. N. McCave, Department of Earth Sciences, University of Cambridge, Downing Street, Cambridge CB2 3EQ, UK.